

Chapter 8

The East African Monsoon System: Seasonal Climatologies and Recent Variations

Chris Funk, Andrew Hoell, Shraddhanand Shukla, Greg Husak
and Joel Michaelsen

Abstract This chapter briefly reviews the complex climatological cycle of the East African monsoon system, paying special attention to its connection to the larger Indo-Pacific-Asian monsoon cycle. We examine the seasonal monsoon cycle, and briefly explore recent circulation changes. The spatial footprint of our analysis corresponds with the “Greater Horn of Africa” (GHA) region, extending from Tanzania in the south to Yemen and Sudan in the north. During boreal winter, when northeast trade winds flow across the northwest Indian Ocean and the equatorial moisture transports over the Indian Ocean exhibit strong westerly mean flows over the equatorial Indian Ocean, East African precipitation is limited to a few highland areas. As the Indian monsoon circulation transitions during boreal spring, the trade winds over the northwest Indian Ocean reverse, and East African moisture convergence supports the “long” rains. In boreal summer, the southwesterly Somali Jet intensifies over eastern Africa. Subsidence forms along the westward flank of this jet, shutting down precipitation over eastern portions of East Africa. In boreal fall, the Jet subsides, but easterly moisture transports support rainfall in limited regions of the eastern Horn of Africa. We use regressions with the trend mode of global sea surface temperatures to explore potential changes in the seasonal monsoon circulations. Significant reductions in total precipitable water are indicated in Kenya, Tanzania, Rwanda, Burundi, Uganda, Ethiopia, South Sudan, Sudan, and Yemen,

C. Funk (✉)

US Geological Survey Center for Earth Resources and Observation (EROS) Center, Reston,
USA

e-mail: chris@geog.ucsb.edu; cfunk@usgs.gov

C. Funk · A. Hoell · S. Shukla · G. Husak · J. Michaelsen

Santa Barbara Climate Hazards Group, University of California, Santa Barbara, CA, USA

e-mail: hoell@geog.ucsb.edu

S. Shukla

e-mail: shrad@geog.ucsb.edu

G. Husak

e-mail: husak@geog.ucsb.edu

J. Michaelsen

e-mail: michaelsen@geog.ucsb.edu

with moisture transports broadly responding in ways that reinforce the climatological moisture transports over the Indian Ocean. Over Kenya, southern Ethiopia and Somalia, regressions with velocity potential indicate increased convergence aloft. Near the surface, this convergence appears to manifest as a surface high pressure system that modifies moisture transports in these countries as well as Uganda, Tanzania, Rwanda, and Burundi. An analysis of rainfall changes indicates significant declines in parts of Tanzania, Rwanda, Burundi, Uganda, Kenya, Somalia, Ethiopia, and Yemen.

Keywords East Africa monsoon system • Precipitation • CHIRPS

8.1 Introduction

For thousands of years, scientists and philosophers have pondered the motions of winds and clouds, and our understanding of monsoons is based on these early foundations. Aristotle was one of the first to put these thoughts to paper. In his *Meteorology* (Aristotle 350 B.C.), he explores the mystery of the atmosphere and meteors, and begins to describe the links between heating, evaporation, and the forces that drive the winds: “The explanation of these and many other phenomena is this. When the sun warms the earth the evaporation which takes place is... of two kinds.... One kind is rather of the nature of vapour, the other of the nature of a windy exhalation. That which rises from the moisture contained in the earth and on its surface is vapour, while that rising from the earth itself, which is dry, is like smoke. Of these the windy exhalation, being warm, rises above the moister vapour, which is heavy and sinks below the other.” While still vague, concepts such as these would evolve into modern meteorology and our modern view of monsoon circulations. The ancient Greeks and Romans used the seasonally reversing Indian trade winds to travel between the Middle East, East Africa, and India (Fig. 8.1). Coined “mawsim” (“timely” and “appropriate”) by Arab traders, these monsoon winds, and the Indo-Pacific circulation that drives them, still strongly influence the climate of food-insecure and drought-prone East Africa.

In this chapter we explore the seasonal variation of the Indo-Pacific monsoon circulation together with the associated climate of East Africa, which we define as the region stretching from Tanzania in the south to Eritrea, Djibouti, and Yemen in the north. Longitudinally, our focus is on food-insecure countries exhibiting monsoonal rains that depend on moisture transports from the Indian Ocean: Tanzania, Rwanda, Burundi, Uganda, Kenya, Somalia, Ethiopia, Djibouti, Eritrea, and Yemen. Our main objectives are to describe the mean seasonal climatological variations across eastern Africa, and to examine recent changes in atmospheric circulation and rainfall.



Fig. 8.1 Seventeenth-century map depicting the locations of the Periplus of the Erythraean Sea. Map created on December 31, 1596, by Abraham Ortelius (1527–1598) for *Periplus Maris Erythraei*, originally written in Greek in the first century CE. A Periplus is an account that lists, in order, coastal ports and landmarks

8.2 Background

The seasonal progression and reversal of the Indian Monsoon circulation (Ramage 1971) modifies East African climate by affecting patterns of moisture transport, subsidence, and precipitation (Riehl 1979). These links can help us understand East Africa’s seasonal cycle, seasonal climate variability, and climate trends. During boreal winter and fall, easterly sub-tropical Indian trade winds in both the Northern and Southern Hemispheres turn rapidly into westerlies over the western Indian Ocean, flowing back to the east at about 5–10°S (Hastenrath et al. 2007, 2011). Since the conservation of angular momentum induces easterly tendencies in most tropical flows, these mean westerly winds are quite remarkable, and can be considered as part of the equatorially-trapped Rossby wave response of the tropical atmosphere to a steady source of heating in the tropical Indo-Pacific Warm Pool (Gill 1980, 1982). From this perspective, warm pool heating drives westerly flows reducing onshore moisture supplies into East Africa, helping to explain the region’s

climatologically dry conditions. As we will see, this classic Gill-Matsuno-like response (Gill 1980, 1982) only holds climatologically during the boreal fall and winter. During the spring and summer, the cross-equatorial monsoonal circulation brings heavy cross-equatorial flows and easterly moisture supplies into Kenya and Ethiopia.

Modulations of Indo-Pacific Warm Pool heating can affect East Africa, either through inter-annual variations such as the El Niño-Southern Oscillation (ENSO) (Camberlin 1995; Camberlin and Philippon 2002; Funk et al. 2013; Hastenrath et al. 2007, 2011; Hoell and Funk 2013a; Hoell et al. 2014; Ogallo et al. 1988; Okoola 1999; Williams et al. 2011; Williams and Funk 2011); the Indian Ocean Dipole (IOD) (Goddard and Graham 1999; Saji et al. 1999); lower frequency warming trends (Cook and Vizy 2013; Funk et al. 2005, 2008, 2013; Hoell and Funk 2013b; Rowell et al. 1995; Williams et al. 2011; Williams and Funk 2011); or Pacific Decadal Variability (Lyon and DeWitt 2012; Lyon et al. 2013; Yang et al. 2014).

What this new research suggests is that Walker circulation-like climate variations are primary drivers of East African drought. As opposed to Hadley circulation analyses, which examine meridional (north-south) circulation averages, the Walker circulation (Bjerknes 1969) looks at zonal (east-west) climate averages taken near the Equator. These averages reveal that very warm regions (the “warm pool”) in and over the eastern Indian and western Pacific Oceans are associated with high rates of precipitation and moisture and heat convergence (Bjerknes 1969). The energy associated with this heavy convection, however, is transported aloft to the eastern Pacific and East Africa, where it can result in subsiding air and low-level high pressure.

Conceptually, this view suggests a more zonal (Walker cell-like) understanding of the drivers of aridity in East Africa and the Sahel climate, as opposed to a focus on a meridional (Hadley circulation-like) progression (Rodwell and Hoskins 1996). It is interesting to note, for example, that a relatively simple hydrostatic primitive equation model, forced with diabatic forcing representing the Asian Monsoon during boreal summer, recreates many important features of the Indo-Asian-African summer climate (Rodwell and Hoskins 1996): the curved cross-equatorial monsoonal winds, and patterns of ascent and subsidence consistent with rainfall maxima over India/East Asia and Sudan/Ethiopia as well as rainfall minima over eastern and southern Africa.

The “Walker Cell” depiction seems to fit East Africa fairly well in boreal fall and winter (Hastenrath et al. 2007), when the mean circulation has a westerly mean, lower level winds over the equatorial Indian Ocean. This changes as the “monsoonal” Somali Jet (Findlater 1969) forms over East Africa during boreal spring and summer. Instead of turning east to form equatorial westerlies over the Indian Ocean, the low level winds cross from the Southern Hemisphere and recurve towards India.

The Somali Jet is thought to arise through the interaction of differential land-ocean heating contrast, the influence of the East African and Madagascar

highlands, and the “beta effect” (Krishnamurti et al. 1976). This jet, one of the most vigorous and constant low-level jet patterns, links the East African and Indian Monsoons (Vizy and Cook 2003). The Somali Jet plays a dual role in the East African climate, providing both a key source of moisture, but also a source of subsidence. Between March and April, as the Somali Jet shifts northward (Findlater 1969), East Africa experiences a rapid “monsoon jump” as the locus of rainfall shifts rapidly from southern to eastern Africa (Riddle and Cook 2008), bringing onshore moisture transports (Viste and Sorteberg 2013) and rapid increases in precipitation during the boreal spring “long” rains. As the zonal branch of the Somali Jet forms during boreal summer, moisture is advected eastward towards the Indian monsoon. Low-level diffuence along the Somali Jet’s westward flank produces subsidence, reducing rainfall across eastern East Africa. These large-scale climate controls, the seasonal migration of warming from insolation, and the local influences of lakes and mountains, combine to produce the extremely complex timing and intensity of East African rainfall (Liebmann et al. 2012).

Given the tremendous complexity of East Africa’s precipitation, it should not be too surprising that considerable uncertainty surrounds projections for East African climate change. In general, the latest coupled ocean-atmosphere simulations produced for the Phase 5 Coupled Model Intercomparison Project (CMIP5) indicate wetter conditions in East Africa (IPCC 2014). These increases in rainfall appear to be at odds with observations of decreased precipitation during boreal spring, which appears to be linked to increases in ocean temperatures and convection over the Indian (Funk et al. 2008, 2005; Verdin et al. 2005) or Indo-Pacific (Funk 2012; Lyon and DeWitt 2012; Williams et al. 2011; Williams and Funk 2011) Oceans. Recent experiments with global atmospheric circulation models (Funk 2012; Funk et al. 2013; Hoell and Funk 2013a, b; Lyon and DeWitt 2012; Yang et al. 2014) suggest that increased western Pacific sea surface temperatures (SST) and SST gradients, as well as enhanced warm pool convection, contribute to more frequent East African droughts.

Some East African mesoscale model simulations also indicate drying (Cook and Vizy 2013). Cook and Vizy (2013) drive the Weather Research and Forecast regional model (WRF) with 32 vertical levels and 90 km resolution. Cook and Vizy contrast WRF simulations forced with 1981–2000 boundary conditions and WRF simulations forced with 2041–2060 boundary conditions derived from nine coupled global climate models. During boreal spring, the difference between these two sets of simulations indicates a weakening Somali Jet, westerlies over the equatorial Indian Ocean, and reduced rainfall over Ethiopia, Somalia, Kenya, and Tanzania. These simulations also indicate an increase in the Arabian high pressure cell.

One likely source of discrepancy between the global CMIP5 model results for East Africa and the results produced by atmospheric global circulation models (AGCMs) and regional models is the tendency for CMIP5 models to predict an increase in El Niño-like SST and precipitation in the central Pacific (Chadwick et al.

2012), while the observed climate has shifted towards El Niño-like warming in the opposite direction (Cane et al. 1997; Compo and Sardeshmukh 2010; L'Heureux et al. 2013; Solomon and Newman 2012). El Niño-like SSTs are anomalously warm in the central and eastern equatorial Pacific.

While it has been suggested that warming in the CMIP5 models in the eastern/central Pacific is tied to a slowing of the global atmospheric circulation (Held and Soden 2006), there is little observational evidence for a corresponding shift towards stronger or more frequent ENSO events (Giese and Ray 2011), and stronger Pacific trade winds appear to have slowed warming in the Eastern Pacific by advecting heat into the extra-tropical Pacific (England et al. 2014). New research suggests that the El Niño-like tendency of the CMIP5 ensembles is primarily a function of the models' weakening zonal Pacific SST gradient (Sandeep et al. 2014), which is caused by preferential warming in the central and eastern equatorial Pacific. This differs substantially from the slowing of global convective mass flux explanation offered by Held and Soden (2006). Using AGCMs driven with ENSO and ENSO-residual SST, Sandeep et al. show that while both components indicate a slowing of global convective mass flux, the ENSO and ENSO-residual components indicate, respectively, a weakening and strengthening of the Walker Circulation, with the latter forcing dominating. In this chapter, we examine observed circulation changes, based on regressions with global "trend mode" SST principal component time series.

8.3 Data

We examine reanalysis fields (Kalnay et al. 1996) from the National Center for Environmental Prediction and the National Center for Atmospheric Research (NCEP/NCAR), precipitation observations from the Climate Hazards Group Infrared Precipitation with Stations (CHIRPS) dataset, and the National Ocean and Atmospheric Administration's Extended Reconstructed sea surface temperatures (NOAA ERSST Smith et al. 2008); we also briefly examine SST from eight CMIP5 simulations (Table 8.1).

The CHIRPS data set is a 30+ year quasi-global rainfall dataset (Funk et al. 2014). Spanning 50°S–50°N (and all longitudes), CHIRPS begins in 1981 and extends to the near present. The data set combines 0.05° resolution satellite imagery with in situ station data to create gridded rainfall time series for trend analysis and seasonal drought monitoring. For East Africa, CHIRPS is comparable (Shukla et al. 2014a) to the research quality Global Precipitation Climatology Centre (GPCC) product (Schneider et al. 2013), but is updated in near real time to support drought early warning applications.

Table 8.1 CMIP5 simulations used in this study

Modeling group and model name	Model acronym	Historical simulations
Canadian Centre for Climate Modelling and Analysis <i>Canadian Earth System Model, version 2</i>	CanESM2	5
National Center for Atmospheric Research <i>Community Climate System Model, version 4</i>	CCSM4	4
Community Earth System Model Contributors <i>Community Earth System Model version with Community Atmospheric Model, version 5</i>	CESM1-CAM5	2
Centre National de Recherches Météorologiques/Centre Européen de Recherche et Formation Avancée en Calcul Scientifique <i>Centre National de Recherches Météorologiques (CNRM) Coupled Global Climate Model, version 5</i>	CNRM-CM5	4
NOAA Geophysical Fluid Dynamics Laboratory <i>Geophysical Fluid Dynamics Laboratory Earth System Model, version 2 with with modular ocean model version 4.1</i>	GFDL-ESM2 M	1
Institut Pierre-Simon Laplace <i>IPSL Community Model version 5</i>	IPSL-CM5A-LR	3
Atmosphere and Ocean Research Institute (University of Tokyo), National Institute for Environmental Studies, and Japan Agency for Marine-Earth Science and Technology <i>Model for Interdisciplinary Research on Climate, version 5</i>	MIROC5	3
Max-Planck-Institut für Meteorologie (Max Planck Institute for Meteorology) <i>MPI Earth System Model Low Resolution</i>	MPI-ESM-LR	3
Total Ensemble		25

8.4 Methods

We seek to better understand links between East African climate and climate change, and variations in the larger scale Indo-Pacific monsoon system. Our analysis focuses first on the mean East African seasonal climate during January–February–March (JFM), April–May–June (AMJ), July–August–September (JAS) and October–November–December (OND). We examine seasonally averaged CHIRPS precipitation and National Center for Atmospheric Research/National Center for Environmental Prediction (NCAR/NCEP) reanalysis: (1) vertically integrated precipitable water; (2) vertically integrated moisture transports; (3) upper tropospheric (0.21 sigma) velocity potential; and (4) divergent wind fields.

We next analyze regressions between integrated precipitable water, moisture transports, velocity potential and divergent wind fields, and the first principal component of global ENSO-residual SST. The empirical orthogonal function

(EOF) associated with this first principal component, hereinafter referred to as the “trend mode,” primarily corresponds to an estimate of the warming in the Indo-Pacific. Several recent studies have examined trends and empirical orthogonal functions (EOFs) of global SST with the influence of ENSO removed (Compo and Sardeshmukh 2010; Solomon and Newman 2012). Removing ENSO-related variations reduces the influence of inter-annual fluctuations and increases the level of agreement among trend fields calculated from different SST data sets.

Here, we have represented ENSO as the first principal component of NOAA Extended Reconstructed (ER) (Smith et al. 2008) tropical Pacific SST (125°E–115°W, 15°S–15°N) over the 1900–2014 time period. Using regression, we isolated and removed 1900–2014 ENSO-related SST variations, then defined the trend mode of variability as the first covariance-matrix-based EOF of global (70°S–70°N) seasonal (JFM, AMJ, JAS, OND) SST anomalies. The 1900–2014 seasonal SST grids were converted to anomalies, weighted by cosine-based weights to account for latitudinal variations in area, and used to compute the covariance matrix and associated eigenvector and principal component. An identical procedure is applied to 25 CMIP5 simulations (Table 8.1) and compared with results obtained from the NOAA ER SST data set.

8.5 The Seasonal Progression of the East African Monsoon

The East African climate is very complex (Liebmann et al. 2012). Over East Africa, the seasonal migration of moisture transports and large-scale patterns of atmospheric convergence and divergence interact with the region’s complex topography to produce patterns of rainfall that can vary by orders of magnitude over hundreds of kilometers. Figure 8.2 shows mean CHIRPS precipitation for JFM, AMJ, JAS, and OND. At the largest scale, there is a clear seasonal progression, as the Inter-tropical Front transitions from a Southern Hemisphere maximum in JFM to a Northern Hemisphere maximum in JAS. The bulk of these rains, however, fall to the southwest or northwest of East Africa. Most of East Africa relies on two relatively meager “bimodal” rainy seasons: the “long rains” during boreal spring (AMJ in this study), and the boreal fall “short rains” (OND).

The seasonal progression of East Africa’s precipitation is largely driven by changes in mean moisture transports and large-scale patterns of subsidence. These changes, in turn, are tightly coupled to seasonal variations in, over, and around the Indian Ocean and western Pacific Warm Pool. We use vertically integrated NCEP/NCAR reanalysis specific humidity (referred to as total precipitable water) and moisture transports to track these seasonal migrations. These moisture transports (Fig. 8.3) closely follow the monsoonal variations of the Indian trade winds. During austral summer (JFM and OND), monsoon winds sweep from the Western Ghat mountains of India towards Somalia. During boreal summer (AMJ and JAS), these winds reverse.

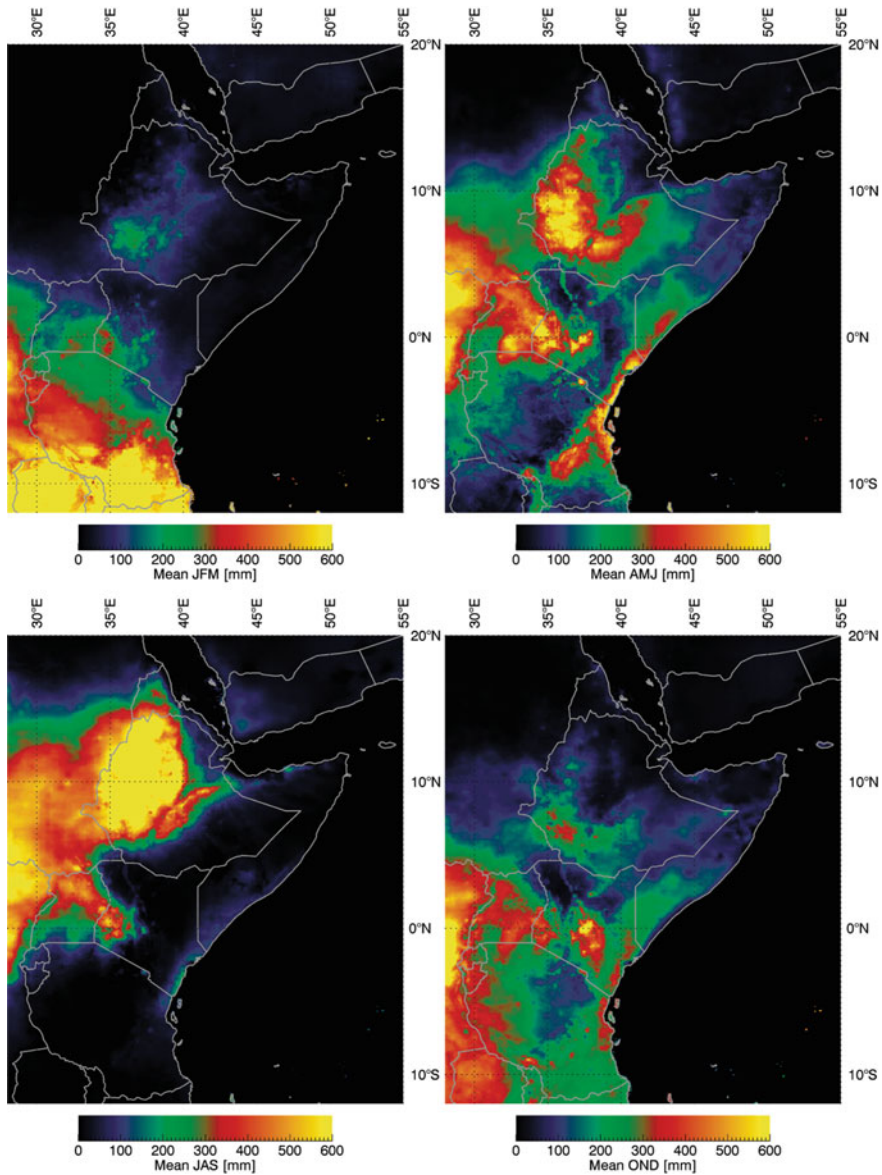


Fig. 8.2 1981–2013 mean CHIRPS

During each season, much of the moisture from the Indian Ocean is redirected to the east before reaching East Africa (Fig. 8.3). In JFM, a strong equatorial westerly jet (Hastenrath et al. 2011) to the northeast of Madagascar helps to drive lower tropospheric convergence and convection over the eastern Indian Ocean and western equatorial Pacific. A surface high pressure resides over Yemen. During AMJ, the

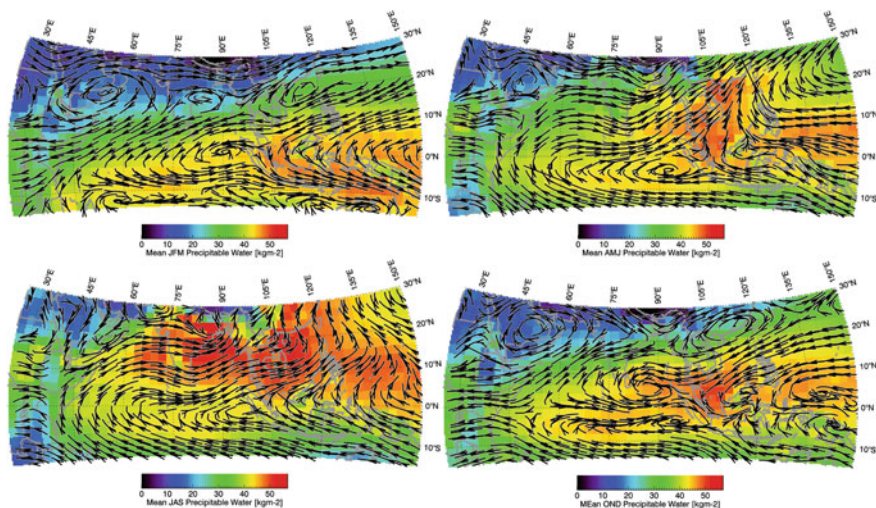


Fig. 8.3 Mean 1981–2010 NCEP/NCAR reanalysis total precipitable water and moisture transports

zonal westerlies over the Indian Ocean weaken, and moisture flows across East Africa, supporting the long rains (Viste and Sorteberg 2013). As these winds cross the Equator, conservation of angular momentum turns them towards India, helping to initiate the Indian Monsoon (Vizy and Cook 2003). As this monsoon intensifies in JAS, the southwesterly Somali Jet across eastern Africa intensifies and shifts eastward, reducing the onshore flow of moisture and producing subsidence across parts of eastern Kenya, southern Ethiopia, and Somalia. During OND, the Indian monsoon subsides and the reversing Indian trades bring moisture to feed the East African short rains. As the surface low pressure system over the south equatorial Indian Ocean intensifies in JFM, these transports diminish, and the seasonal cycle repeats. The seasonal cycle of East African climatology, therefore, is tightly coupled to the tropical Indo-Pacific and Indian Monsoon circulations.

The Indo-Pacific and Indian Monsoon circulations help create the conditions that give much of East Africa a semi-arid or arid climate. In general, East Africa does not receive bountiful rains because low pressure, along with temperature and moisture convergence over the warm equatorial Indo-Pacific, pull the bulk of the moisture transports to the east. This has long been understood as part of the “Walker circulation,” first described by Bjerknes (1969), and named after the British meteorologist Sir Gilbert Walker, who first described the Southern Oscillation (Walker 1923). Following Bjerknes (1969), Fig. 8.4 shows a schematic diagram of the east-west (zonal) circulation. The bottom of the figure represents the earth’s surface, and the top of the diagram, the tropopause. The left of the image describes the climatological conditions typical for much of East Africa. In the upper troposphere, winds converge into an area of upper-level low geopotential heights, producing subsidence. This subsidence reinforces a high pressure cell near the

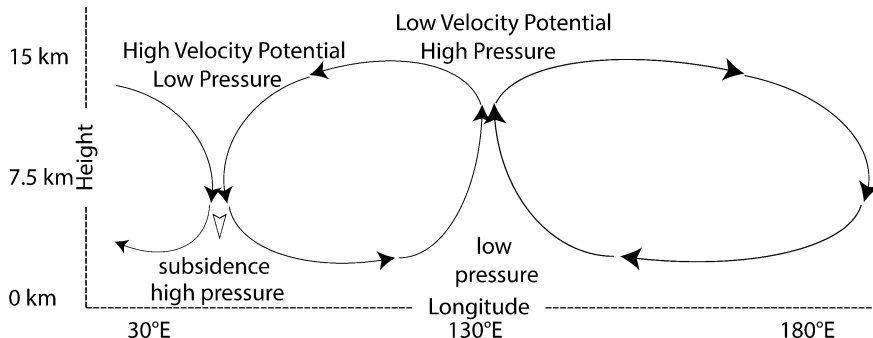


Fig. 8.4 Height by longitude schematic describing velocity potential

surface, which in turn supports low-level moisture divergence and dry conditions. Over the eastern Indian Ocean and western Pacific (located in the center of our schema), conditions are reversed, producing a convergence of moisture and heat, increasing the moist static energy and driving large-scale convection and precipitation. The convergence of latent and sensible heat increase geopotential heights aloft, producing an upper-level high.

These types of circulation features can be effectively visualized using a “velocity potential” field; this is a scalar field defined such that the divergent (non-geostrophic) wind field flows along (perpendicular to) the velocity potential field, flowing from low-velocity potential regions to high-velocity potential areas. Thus, near the Equator, the upper-level divergent wind will flow from an area of high geopotential heights, and low-velocity potential to areas of low geopotential heights and high velocity potential. Figure 8.5 shows climatological velocity potential and divergent wind streamlines for East Africa, estimated near the top of the tropopause (the 0.21 sigma \approx level 200 hPa).

Figure 8.5 gives us additional insight into the march of seasons that drives the various stages of the East African monsoon. In general, in each season we find low-velocity potentials over the Indian Ocean and higher velocity potentials over East Africa (this intensifies during JAS). These velocity potential gradients are associated with easterly divergent winds. During JFM and JAS, these upper-level winds converge, respectively, over North Africa and the Middle East and over Southern Africa. During AMJ and JAS, upper-level convergence weakens over Sudan and the rest of the Sahel, and upper-level conditions are fairly conducive to rainfall over Yemen and most of East Africa. During OND, strong upper-level convergence stretches from eastern Tanzania across Kenya, eastern Ethiopia, and Yemen. While the Middle East is already under the influence of a low-level high pressure cell (Fig. 8.3), East Africa, during the OND “short rains,” receives onshore moisture transports from over the northeast Indian Ocean. When El Niño (Indeje et al. 2000) or positive Indian Ocean Dipole (IOD) events (Saji et al. 1999) affect the zonal Indo-Pacific circulation, the region can experience heavy OND rainfall.

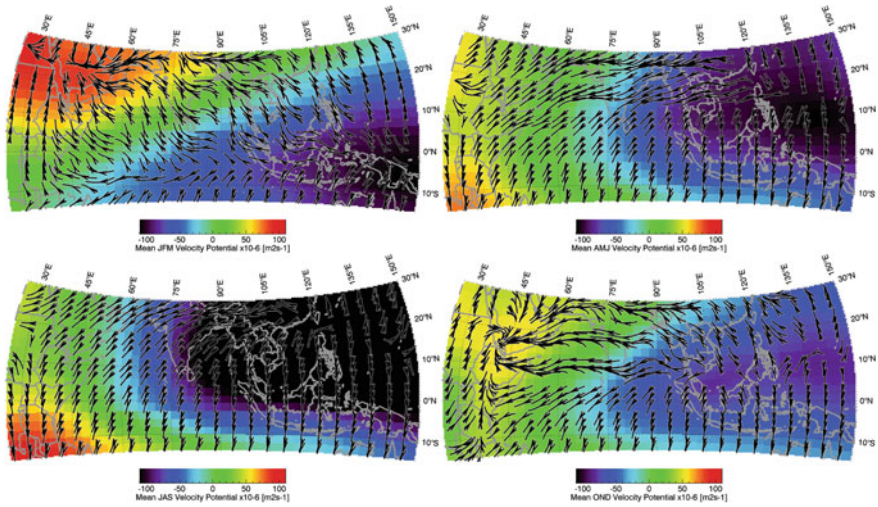


Fig. 8.5 Mean 1981–2010 NCEP/NCAR reanalysis 0.21 sigma velocity potential heights and divergent wind fields

In addition to large-scale circulation controls, the East African climate is also heavily influenced by local topography and Lake Victoria. The influence of these features can create great changes in mean climate over short distances. In general, rainfall at higher elevations is typically much higher than at lower elevations. Air temperatures exhibit an inverse relationship; thus much of East Africa contains hot, dry lowlands interspersed with cool, wet highland areas. Food-insecure populations and environments can often be found along the edges of these gradients, in between the very wet regions that receive consistent rains, and the arid lands that are consistently dry.

8.6 Relating Circulation Trends to Large-Scale Warming Patterns

The next section of this chapter will examine the relationship between the regional circulation and large-scale warming trends. We use total precipitable water and moisture transports to represent the lower atmosphere. The upper atmosphere is represented by upper-level (0.21 sigma) velocity potential fields. We examine trends in these fields by regressing them against the first principal component of global sea surface temperatures, after the influence of ENSO has been removed. We refer to this as the “trend mode” of global SST. While the overall SST trends and atmospheric responses in the CMIP5 models tend to represent an El Niño-like shift in the mean climate (Chadwick et al. 2012), this tendency appears to be closely related to the CMIP5 model’s tendency to warm SSTs in the eastern Pacific more

rapidly than in the western (Sandeep et al. 2014). While both observations and the CMIP5 simulations indicate a warming central and eastern Pacific, the magnitude of the CMIP5 warming is substantially greater. We can see this by examining principal component time series (Fig. 8.6) and eigenvectors calculated over the 1900–2013 seasonal (AMJ) tropical Pacific (125°E – 65°W , 15°S – 15°N) SST in the NOAA ER SST observations and our CMIP5 ensemble (Table 8.1). While the overall magnitude and timing of the observed and CMIP5-simulated time series (Fig. 8.6a) is quite similar (except for decadal fluctuations in the observations about the CMIP5 ensemble mean), the CMIP5 ENSO response, as represented by the CMIP5 eigenvectors (Fig. 8.6b), is much greater. Together, Fig. 8.6a, b suggest that the CMIP5 models over-estimate the strength of warming in the eastern equatorial Pacific. This warming, and the resulting change in SST gradients, seem to be largely responsible for the slowing of the CMIP5 Walker Circulation.

Here, we focus on the empirical relationships between the NCEP/NCAR reanalysis and the observed trend mode first principal component. The observed and CMIP5 modeled trend mode changes are substantially more congruent than changes related to ENSO. As described in the background section, this ENSO-residual “trend mode” isolates a component of large-scale climate variability (the non-ENSO warming trend) that appears consistent across datasets (Cane et al. 1997; Compo and Sardeshmukh 2010; Solomon and Newman 2012).

Figure 8.7a shows the recent annual trend mode SST changes between 1999–2013 and 1979–1998, based on observed data (the NOAA ER SST). The 1999–2013 and 1979–1998 break periods were chosen to correspond with recent analyses describing a “Pacific Shift” in SST (Lyon et al. 2013). One key characteristic of the observed trend mode SST, the stronger western-to-central Pacific equatorial SST

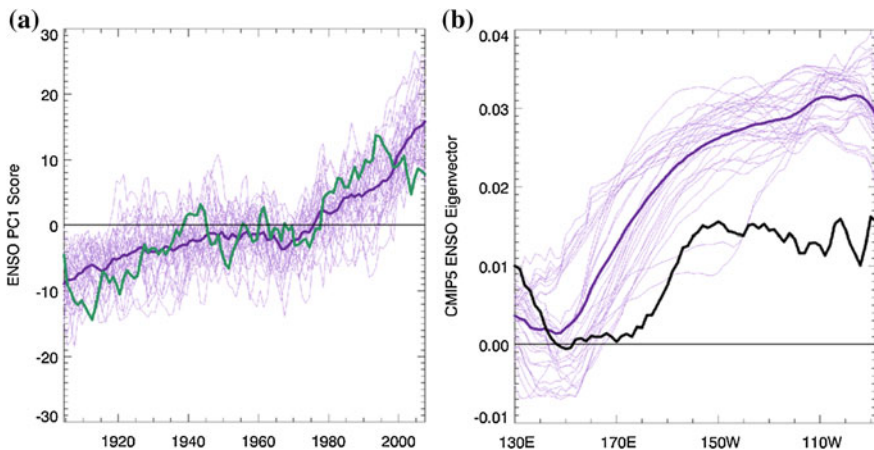


Fig. 8.6 **a** Ten-year averaged time series of observed (blue) and simulated CMIP5 (purple) ENSO principal component scores. **b** Meridionally averaged eigenvectors of tropical Pacific SST (15°S – 15°N). In both **a** and **b**, individual simulations are shown with thin purple lines, while the thick purple lines indicate the ensemble averages

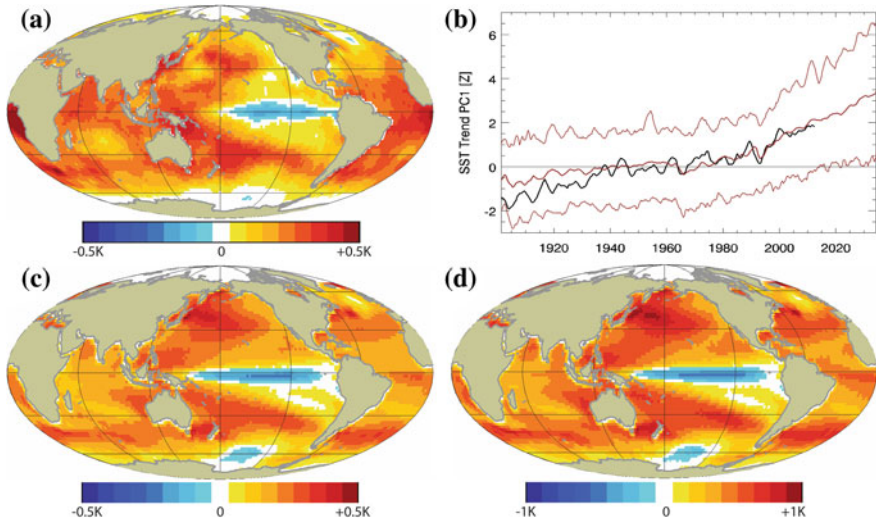


Fig. 8.7 **a** Change in SST associated with the observed trend mode between 1999–2013 and 1979–1998. **b** Time series of standardized observed and CMIP5 trend mode PCs, together with the minimum and maximum CMIP5 PC scores. **c** CMIP5 ensemble mean trend mode changes between 1999–2013 and 1979–1998. **d** Same as **c**, but for 2026–2035 compared to 1979–1998

gradient, has been described in a number of ENSO-residual trend studies, beginning with Cane et al. (1997), followed by Compo and Sardeshmukh (2010) and Solomon and Newman (2012). These stronger gradients tend to reduce the long rains over East Africa (Liebmann et al. 2014) and intensify the impacts of La Niña events (Hoell and Funk 2013a; Hoell et al. 2014), contributing to the greater rainfall deficits associated with more modern La Niña conditions (Williams and Funk 2011). Warming in the equatorial Indian Ocean (Funk et al. 2008) and western Pacific (Funk 2012) track very closely with CMIP5 SST predictions, and these warm waters have warmed substantially over the last 30 years.

The timing of the observed and CMIP5-estimated changes in the smoothed (10 year running mean) trend mode principal component scores is shown in Fig. 8.7b. While the minima-to-maxima spread of CMIP5 ensemble is quite large, the ensemble mean tracks very closely with the observed NOAA ER principal component time series. Both the observations and CMIP5 simulations indicate substantial increases between 1979 and 2013. Figure 8.7c combines the changes in these principal components with the CMIP5 eigenvectors to produce estimates of 1999–2013 versus 1979–1998 trend mode SST changes. Both the observations (Fig. 8.7a) and models (Fig. 8.7b) indicate substantial warming in the equatorial western Pacific and sub-tropics. The CMIP5 ENSO-residual trend mode also expresses slight cooling in the central Pacific, consistent with prior ENSO-residual empirical trend analyses (Cane et al. 1997; Compo and Sardeshmukh 2010; Solomon and Newman 2012).

By 2026–2035, continued trend mode warming could lead to even greater warming in the western equatorial Pacific (Fig. 8.7d), where climatological SSTs exceed 29 °C. SST patterns similar to Fig. 8.7a, b, d have been shown to produce drying across eastern Africa (Lyon and DeWitt 2012), and continued warming along these lines could intensify convection and precipitation over the warm pool, potentially influencing the monsoon circulations over East Africa.

We next use regressions between seasonal trend mode principal components (derived from the 1900–2013 NOAA ER SST) and NCEP/NCAR reanalysis total precipitable water, moisture transports, upper troposphere (0.21 sigma) velocity potential, and divergent wind fields to explore potential changes in the East African monsoon. Figure 8.8 shows the seasonal moisture and moisture transport regressions. Statistical significance in the figures is estimated at $p = 0.1$, based on a two-sided t-test with 64 degrees of freedom. Figure 8.9 contains similar seasonal velocity potential regression maps. The seasonal responses vary substantially, yet also indicate interesting similarities.

8.6.1 Seasonal Similarities for Sudan and Western Ethiopia

During all seasons, and particularly during JFM, the precipitable water regressions (Fig. 8.8) suggest atmospheric moisture declines in two primary locations: (1) across eastern Kenya, Tanzania, and Ethiopia, and southern Somalia, and

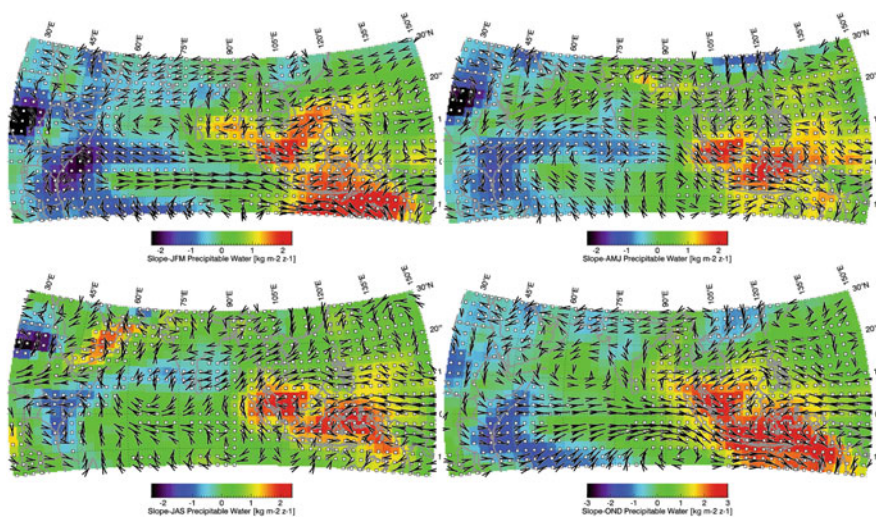


Fig. 8.8 1948–2013 regression between the trend mode first principal component and NCEP/NCAR reanalysis total precipitable water and moisture transport fields. Velocity potential slopes not significant as $p = 0.1$ were set to 0

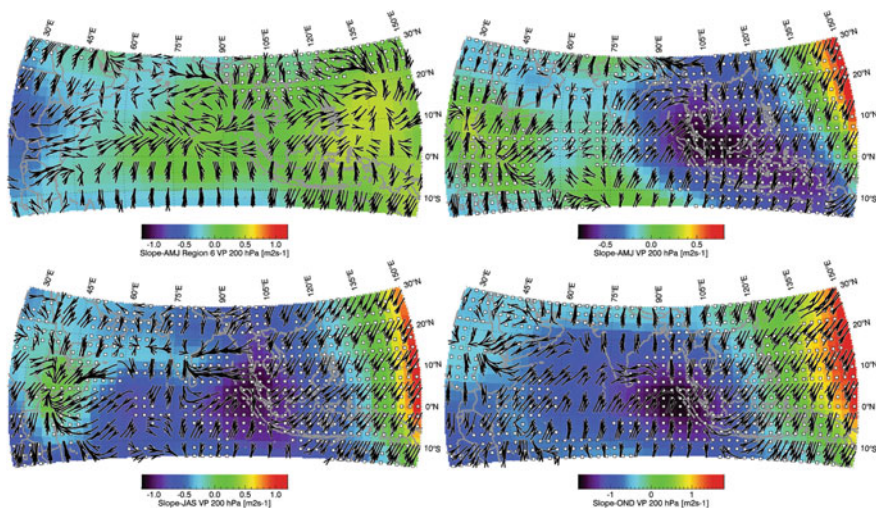


Fig. 8.9 1948–2013 regression between the trend mode first principal component and NCEP/NCAR reanalysis 0.21 sigma velocity potential heights and divergent wind fields. Velocity potential slopes not significant at $p = 0.1$ were set to 0

(2) across Sudan. The negative relationship to Sudan’s total precipitable water appears related to a near surface high pressure cell, and anticyclonic circulation patterns that increase dry northerly transports while reducing moist flows out of the Congo basin. This region (and far western Ethiopia) has been found to be associated with 1990–2009 versus 1960–1989 rainfall declines during the main boreal summer rainy seasons, and appears to exhibit some of the most dramatic warming rates in East Africa and the Sahel (Funk et al. 2012). More discussion of the disruption of Congo moisture transports can be found in Williams et al. (2011), Jury and Funk (2012), and Viste and Sorteberg (2013). This surface high pressure cell and associated anticyclonic moisture transport responses appears to be supported by upper-level convergence in the divergent wind field responses (Fig. 8.9). In JFM and OND, the velocity potential response appears broadly similar to the velocity potential climatology; the response to the long-term warm trend (as represented by the trend principal component) may act to exacerbate the meridional (north-south) velocity potential gradient between the Sahara and southern Africa. Such a pattern would be associated with more (less) subsidence over the Sahara (southern Africa). The velocity potential regressions appear more complicated during AMJ and JAS. During AMJ and JAS, the climatological upper level divergent winds (Fig. 8.5) over Africa reverse, blowing into southern Africa and resembling the converse of the low-level monsoon trades across the northeast Indian Ocean (Fig. 8.3). During these seasons, the pattern of upper-level convergence (and increasing velocity potential) over Sudan appears to merge with subsidence over Ethiopia, Somalia, and Kenya.

8.6.2 Seasonal Similarities for Kenya, Tanzania, Somalia and Southern Ethiopia

We will now briefly discuss the seasonal moisture and velocity potential responses in “eastern East Africa,” i.e., portions of Kenya, Tanzania, Somalia, and Ethiopia. While substantial declines in total precipitable water are indicated in each season, the spatial structure of the moisture transport responses varies substantially. During JFM and OND, the mean moisture flow across the Indian Ocean is the most zonal (Fig. 8.3), and one finds very large westerly mean transports between 5°N and 10°S. The trend mode responses during these boreal winter seasons (Fig. 8.8) resemble the climatological flows over the Indian Ocean (Fig. 8.3). During boreal winter, the link between these zonal winds and East African drought is well established (Hastenrath et al. 2011), and there is a strong link between El Niño (La Niña) and increased (decreased) East African rainfall. The low frequency trend mode principal component appears consistent with a La Niña-like change in boreal winter moisture transports.

As the Indian monsoon begins during the late portion of AMJ, the structure of both mean moisture transports (Fig. 8.3) and moisture transport responses (Fig. 8.8) change dramatically. Climatologically, ridging over the northwest Indian Ocean weakens, and monsoon trade winds cross into the Northern Hemisphere and recurve to the east, conserving angular momentum. Over the western Indian Ocean, the AMJ and JAS moisture transport responses appear to reinforce these climatological conditions. The southerly trade winds, and their local East African counterpart (the Somali Jet) are divergent along their western flanks, and this may be exacerbated by the intensified monsoonal trade patterns indicated during AMJ and JAS in Fig. 8.8. In the upper troposphere, in boreal spring and summer, we find strong upper-level convergence over Kenya, Ethiopia, Somalia and South Sudan, consistent with higher surface pressures.

8.7 Changes in CHIRPS Precipitation

We conclude with a brief examination of recent changes in CHIRPS precipitation (Fig. 8.10), which shows the recent (1999–2013 vs. 1981–1998) changes in standardized seasonal CHIRPS precipitation. Locations without significant ($p = 0.1$) precipitation changes or climatological precipitation with a standard deviation of <10 mm are not shown. Significance was estimated via a two-sided difference-of-means t-test. There has been a recent (1998) shift in Pacific SSTs that is thought to impact East African rainfall; we therefore examine here the differences in 1998–2013 and 1981–1997 mean rainfall. These changes have been divided by the 1981–2013 standard deviation to show changes in standardized precipitation. Changes not significant at $p = 0.1$ are not shown as a values in regions with seasonal rainfall standard deviations of <10 mm.

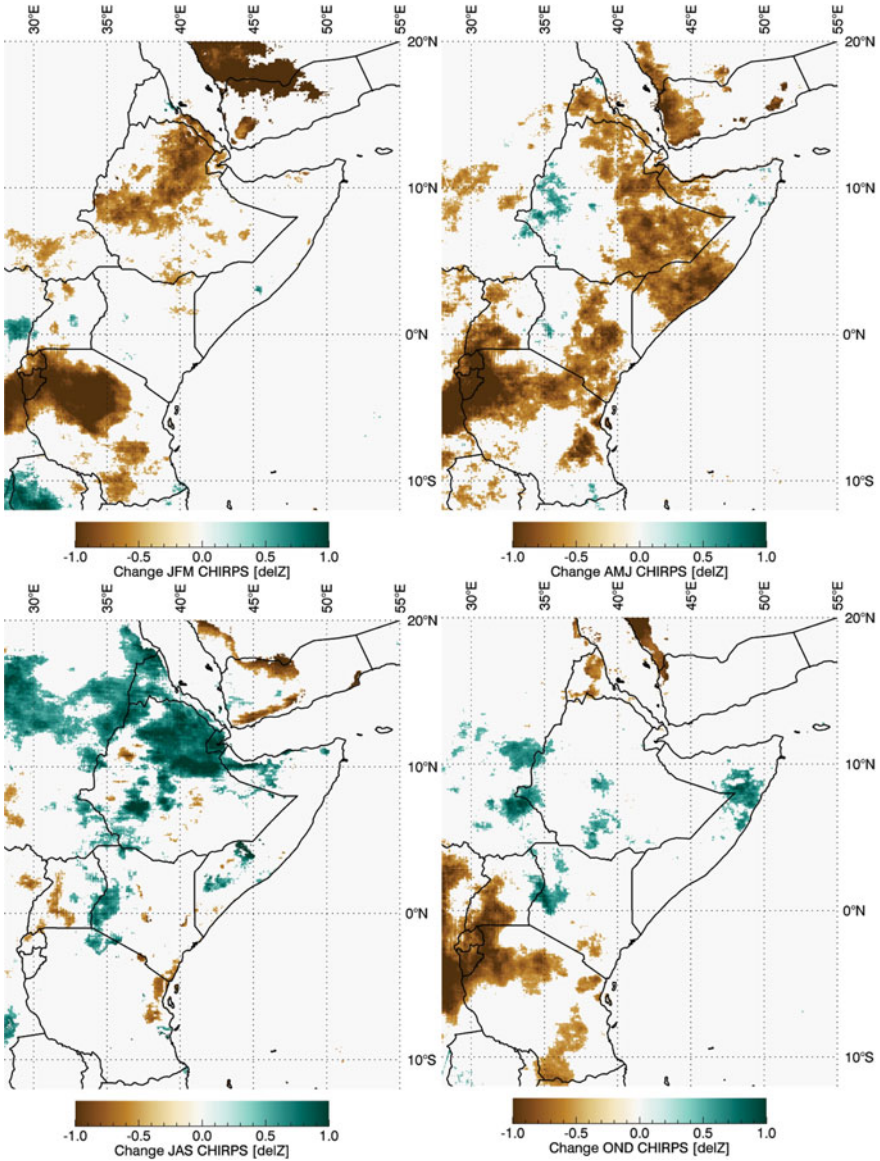


Fig. 8.10 Change in CHIRPS mean precipitation between 1998–2013 and 1981–1997, expressed in standardized deviations. Changes not significant at $p = 0.1$, based on a two-sided difference of means t-test, have been set to zero

During JFM, substantial drying is identified in Tanzania, Rwanda, Burundi, northern Ethiopia, and parts of the Middle East. The changes in Tanzania, Rwanda, and Burundi are probably much more significant, given the importance of this season climatologically. This region, in fact, exhibits substantial drying also in AMJ

and OND (i.e., all the seasons in which it typically receives rainfall). While the spatial agreement is not perfect, the reanalysis (Fig. 8.8) does indicate significant reductions in total precipitable water and onshore moisture transports in these seasons as well. In the CHIRPS data, this drying appears associated with rainfall reductions in Uganda in AMJ and OND as well. As suggested by Cook and Vizy (2013), drying in this region appears linked to changes in total precipitable water.

Kenya-Ethiopia-Somalia rainfall changes during AMJ, on the other hand, seem likely to be tied to changes in the Somali Jet, moisture supplies, and subsidence. If the Somali Jet has intensified, as suggested by Fig. 8.8, then dry boreal summer conditions may be arriving earlier in eastern Kenya, Ethiopia, and Somalia, resulting in more frequent droughts. Linking these droughts to enhanced Pacific SST gradients (Liebmann et al. 2014) may create opportunities for prediction (Shukla et al. 2014b).

During JAS, both the reanalysis moisture fields (Fig. 8.8) and CHIRPS precipitation (Fig. 8.10) show substantial increases across northern Ethiopia, as previously noted (Funk et al. 2012; Viste et al. 2012; Williams et al. 2011). Given that the large-scale circulation changes (Fig. 8.9) indicate upper-level convergence, this increase in precipitation appears associated with the lower troposphere. Changes in JAS total precipitable water and moisture transports indicate a strengthening of the Afar convergence zone, which stretches from the northern Ethiopian highlands to Yemen (Viste and Sorteberg 2013); the greatest moisture supply into northern Ethiopia comes from the north, and an intensified Afar convergence zone and associated low pressures would increase these flows. Across southern Ethiopia, the JAS transport regressions indicate an easterly shift, presumably increasing moisture transports into the highlands.

8.8 Conclusions

This chapter has briefly reviewed the complex climatological cycle of the East African monsoon system, paying special attention to its connection to the larger Indo-Pacific-Asian monsoon cycle. This perspective helps explain why parts of East Africa are dry, and why some of these locations are getting drier. The seasonal stage of the Indian monsoon system strongly influences moisture transports. When the winds across the northeast Indian Ocean reverse, the larger pattern transforms dramatically.

During “austral” summer (OND and JFM), cross-equatorial moisture transports are limited, and the key feature (over the Indian Ocean) is a strong westerly jet near the Equator (Hastenrath et al. 2011) that is caused by warm pool convection (Gill 1980, 1982) and modulated by ENSO. During OND, as the Intertropical Convergence Front moves quickly south, Indian trade winds from both the Northern and Southern Hemispheres converge over eastern Africa, and the region experiences its “short” rainy season. The climatological upper level velocity potential for this season, however, tends to produce convergence over the Greater

Horn of Africa, which may help explain this season's high variability and tele-connectivity. For Kenya and Ethiopia, there seems to be little recent change in OND rainfall. OND rainfall changes also seem to be model-dependent. For example, Hoell and Funk (2013) found substantial OND declines in simulations with the Global Forecast System model. On the other hand, Liebmann et al. (2014) found increases. The interpretation provided in the Liebmann study was that the short rains were influenced positively by warming in the northern Indian Ocean but also negatively by warming in the western Pacific, with the former having a slightly stronger influence.

During AMJ and JAS, the South Asian Monsoon begins, and the moisture transport patterns change dramatically. The jet over the equatorial Indian Ocean disappears, and the southeasterly trade winds sweep north across the eastern Indian Ocean and East Africa. For parts of eastern East Africa, these winds bring both a blessing and a burden. Forming the Somali Jet, they bring moisture onshore. This jet, however, produces subsidence on its westward flank, suppressing rainfall. The most bountiful rains occur in the west or at higher elevations, where orographic processes produce uplift. During AMJ, moisture transport regressions indicate stronger southerly monsoon winds at about 50°E; subsidence to the west (over East Africa) might be supported both by these low-level changes in the monsoon winds and upper-level changes in velocity potential and divergent wind fields. Across the southern Middle East, lower-level geopotential heights seem to be rising, and rainfall has also declined in Eritrea, Yemen, and Djibouti. During JAS, however, the Afar convergence zone appears to be intensifying, potentially adding to moisture transports into northern Ethiopia, where rainfall has been increasing.

One compelling result, identified in all seasons, is a tendency towards lower total precipitable water in Tanzania, Kenya, and Somalia. This seems to indicate a low-level ridging tendency. Focusing on Tanzania, Rwanda, Burundi, and Uganda, we see that these countries exhibit substantial rainfall declines during OND, AMJ, and JFM. One likely contributor to these precipitation decreases would be reduction in the onshore transports that typically flow onshore south of the Equator. Ridging tendencies between 10°S and the Equator appear to be reducing these flows in all seasons.

The future of the East African climate is and will be uncertain, given the incredible complexity of the processes that drive both mean and anomalous weather. More and better modeling studies will be needed. This brief chapter has emphasized the connection of East Africa's climate with the South Asian Monsoon and the Walker Circulation, connections that may help us better understand both the mean climate and recent changes in that climate. The results presented here suggest that a strengthening of the Walker circulation (as represented by the first principal component of global SSTs) influences the East African climate in complex but significant ways. Continued monitoring, modeling, and analysis will help us better identify, interpret, and predict those changes.

References

- Aristotle (350 B.C.) *Meteorology*
- Bjerknes J (1969) Atmospheric teleconnections from the equatorial Pacific. *Mon Weather Rev* 97:163–172
- Camberlin P (1995) June–September rainfall in North-Eastern Africa and atmospheric signals over the tropics: a zonal perspective. *Int J Climatol* 15:773–783
- Camberlin P, Philippon N (2002) The East African March–May rainy season: associated atmospheric dynamics and predictability over the 1968–97 period. *J Clim* 15:1002–1019
- Cane MA et al (1997) Twentieth-century sea surface temperature trends. *Science* 275:957–960
- Chadwick R, Boutle I, Martin G (2012) Spatial patterns of precipitation change in CMIP5: why the rich do not get richer in the tropics. *J Clim* 26:3803–3822
- Compo GP, Sardeshmukh PD (2010) Removing ENSO-related variations from the climate record. *J Clim*. doi:[10.1175/2009JCLI2735.1](https://doi.org/10.1175/2009JCLI2735.1), 1957–1978
- Cook KH, Vizy EK (2013) Projected Changes in East African rainy seasons. *J Clim* 26:5931–5948
- England MH et al (2014) Recent intensification of wind-driven circulation in the Pacific and the ongoing warming hiatus. *Nat Clim Change*
- Findlater J (1969) A major low-level air current near the Indian Ocean during the northern summer. *Quart J R Meteorol Soc* 95:362–380
- Funk C (2012) Exceptional warming in the Western Pacific-Indian Ocean warm pool has contributed to more frequent droughts in Eastern Africa. *Bull Am Meteorol Soc* 7:1049–1051
- Funk C, Michaelsen J, Marshall M (2012) Mapping recent decadal climate variations in precipitation and temperature across Eastern Africa and the Sahel. In: Wardlow B, Anderson M, Verdin J (eds) *Remote sensing of drought: innovative monitoring approaches*. CRC Press, p 25
- Funk C, Dettinger MD, Michaelsen JC, Verdin JP, Brown ME, Barlow M, Hoell A (2008) Warming of the Indian Ocean threatens eastern and southern African food security but could be mitigated by agricultural development. *Proc Natl Acad Sci USA* 105:11081–11086
- Funk C et al (2005) Recent drought tendencies in Ethiopia and equatorial-subtropical eastern Africa
- Funk C et al (2013) Attribution of 2012 and 2003–12 rainfall deficits in eastern Kenya and southern Somalia. *Bull Am Meteorol Soc* 94:45–48
- Funk C et al (2014) A quasi-global precipitation time series for drought monitoring 832, p 4
- Gill AE (1980) Some simple solutions for heat-induced tropical circulation. *Quart J R Meteorol Soc* 106:447–462
- Gill AE (1982) *Atmosphere-ocean dynamics*, vol 30. Academic Press, 662 pp
- Giese BS, Ray S (2011) El Niño variability in simple ocean data assimilation (SODA), 1871–2008. *J Geophys Res Oceans* 1978–2012:116
- Goddard L, Graham NE (1999) Importance of the Indian Ocean for simulating rainfall anomalies over eastern and southern Africa. *J Geophys Res* 104:19099–19116
- Hastenrath S, Polzin D, Mutai CC (2007) Diagnosing the 2005 drought in equatorial East Africa. *J Clim* 20:4628–4637
- Hastenrath S, Polzin D, Mutai C (2011) Circulation mechanisms of Kenya rainfall anomalies. *J Clim* 24:404–412
- Held IM, Soden BJ (2006) Robust responses of the hydrological cycle to global warming. *J Clim* 19:5686–5699
- Hoell A, Funk C (2013a) The ENSO-related West Pacific Sea surface temperature gradient. *J Clim* 26
- Hoell A, Funk C (2013b) Indo-Pacific sea surface temperature influences on failed consecutive rainy seasons over eastern Africa. *Clim Dyn* 1–16
- Hoell A, Funk C, Barlow M (2014) La Nina Diversity and the Forcing of Northwest Indian Ocean Rim Teleconnections. *Clim Dyn*

- Indeje M, Semazzi FH, Ogallo LJ (2000) ENSO signals in East African rainfall seasons. *Int J Climatol* 20:19–46
- IPCC (2014) Climate change 2014: impacts, adaptation, and vulnerability. Part B: regional aspects. Contribution of working Group II to the fifth assessment report of the intergovernmental panel on climate change. Cambridge University Press
- Kalnay E et al (1996) The NCEP/NCAR 40-year reanalysis project. *Bull Am Meteorol Soc* 77:437–471
- Krishnamurti TN, Molinari J, Pan HL (1976) Numerical simulation of the Somali jet. *J Atmos Sci* 33:2350–2362
- L'Heureux ML, Lee S, Lyon B (2013) Recent multidecadal strengthening of the Walker circulation across the tropical Pacific. *Nat Clim Change*
- Lyon B, DeWitt DG (2012) A recent and abrupt decline in the East African long rains. *Geophys Res Lett* 39(2). L02702
- Lyon B, Barnston AG, DeWitt DG (2013) Tropical Pacific forcing of a 1998–1999 climate shift: observational analysis and climate model results for the boreal spring season. *Clim Dyn* 1–17
- Liebmann B et al (2012) Seasonality of African precipitation from 1996 to 2009. *J Clim* 25:4304–4322
- Liebmann B et al (2014) Understanding recent Eastern horn of Africa rainfall variability and change. *J Clim* (in press)
- Ogallo LJ, Janowiak JE, Halpert MS (1988) Teleconnection between seasonal rainfall over East Africa and global sea surface temperature anomalies. *J Meteorol Soc Jpn* 66:807–822
- Okoola RE (1999) A diagnostic study of the eastern Africa monsoon circulation during the Northern Hemisphere spring season. *Int J Climatol* 19:143–168
- Ramage C (1971) Monsoon meteorology, vol 296. Academic, San Diego
- Riddle EE, Cook KH (2008) Abrupt rainfall transitions over the greater horn of Africa: observations and regional model simulations. *J Geophys Res Atmos* 1984–2012:113
- Riehl H (1979) Climate and weather in the tropics. Academic Press, UK
- Rodwell MJ, Hoskins BJ (1996) Monsoons and the dynamics of deserts. *Quart J R Meteorol Soc* 122:1385–1404
- Rowell DP, Folland CK, Maskell K, Ward MN (1995) Variability of summer rainfall over tropical north Africa (1906–92): observations and modelling. *Quart J R Meteorol Soc* 121:669–704
- Saji NH, Goswami BN, Vinayachandran PN, Yamagata T (1999) A dipole mode in the tropical Indian Ocean. *Nature* 401:360–363
- Sandeep S, Stordal F, Sardeshmukh P, Compo G (2014) Pacific Walker circulation variability in coupled and uncoupled climate models. *Clim Dyn* 43:103–117
- Schneider U, Becker A, Finger P, Meyer-Christoffer A, Ziese M, Rudolf B (2013) GPCC's new land surface precipitation climatology based on quality-controlled in situ data and its role in quantifying the global water cycle. *Theor Appl Climatol* 1–26
- Shukla S, Funk C, Hoell A (2014) Using constructed analogs to improve the skill of March–April–May precipitation forecasts in equatorial East Africa. *Environ Res Lett* 9.9:094009
- Shukla S, McNally A, Husak G, Funk C (2014) A seasonal agricultural drought forecast system for food-insecure regions of East Africa. *Hydrol Earth Syst Sc* 18(10):3907–3921
- Smith TM, Reynolds RW, Peterson TC, Lawrimore J (2008) Improvements to NOAA's historical merged land-ocean surface temperature analysis (1880–2006). *J Clim* 21:2283–2296
- Solomon A, Newman M (2012) Reconciling disparate twentieth-century Indo-Pacific ocean temperature trends in the instrumental record. *Nat Clim Change* 2:691–699
- Verdin J, Funk C, Senay G, Choularton R (2005) Climate science and famine early warning. *Philos Trans R Soc B* 360:2155–2168
- Viste E, Sorteberg A (2013) Moisture transport into the Ethiopian highlands. *Int J Climatol* 33:249–263
- Viste E, Korecha D, Sorteberg A (2012) Recent drought and precipitation tendencies in Ethiopia. *Theor Appl Climatol* 112:535–551
- Vizy EK, Cook KH (2003) Connections between the summer East African and Indian rainfall regimes. *J Geophys Res Atmos* 108:4510

- Walker GT (1923) Correlation in seasonal variations of weather, VIII. A Preliminary study of world weather. *Memoirs of the Indian Meteorological Department*
- Williams P, Funk C (2011) A westward extension of the warm pool leads to a westward extension of the walker circulation, drying eastern Africa. *Clim Dyn*
- Williams A et al (2011) Recent summer precipitation trends in the greater horn of Africa and the emerging role of Indian Ocean sea surface temperature. *Clim Dyn* 1–22
- Yang W, Seager R, Cane MA, Lyon B (2014) The East African long rains in observations and models. *J Clim*